Self-Organized Network of Chemical Reactions: A Model of Contaminated Converging and Diverging Flows in Fractured Media†

Randall A. LaViolette*

Idaho National Engineering & Environmental Laboratory, Idaho Falls, Idaho 83415-2208

Robert J. Glass

Sandia National Laboratories, Albuquerque, New Mexico 87185-0735

David Peak

Department of Physics, Utah State University, Logan, Utah 84322-4415

Daphne L. Stoner

Department of Chemistry, University of Idaho, Idaho Falls, Idaho 83402

Received: May 31, 2004; In Final Form: September 9, 2004

A self-organized "tipping bucket model" of driven flow in fractured media was employed to study the degradation of contaminant by a dynamic population of traps representing microbial activity in the subsurface. For divergent flows, an increase in the degradation rate by an order of magnitude decreased the contaminant concentration in the exiting drips by at most one-third, but for convergent flows, the increased degradation rate did not significantly reduce the contaminant concentration.

1. Introduction

The fate of contaminants (e.g., halocarbons) in the subsurface, especially in the vadose zone (i.e., the unsaturated zone above groundwater), remains a challenge to predict. Among the complications is the possibility of nonlinear feedback between the transport and in-situ degradation of the contaminants. Contaminants spilled into the vadose zone may react with and be degraded by communities of native microorganisms resident throughout the vadose zone, which may themselves also impact the flow of contaminants.[1] Theoretical (i.e., statistical mechanics) and computational studies[2,3] of the reaction−diffusion equations that describe microbial degradation of contaminants (which were introduced only once into a diffusive flow in a saturated porous medium, with a static population of degradation sites) found that the disorder in the spatial distribution of the degradation sites strongly influenced the degradation kinetics. Here, we studied a model of the degradation of contaminants continually introduced into a driven flow in fractured nonporous unsaturated media, combined with a dynamic population of microbial degradation sites. This model is the "tipping bucket model" (TBM), introduced in refs 4 and 5. The TBM is a variant of the scale-free "sandpile" model of self-organized criticality.[6] In the TBM, the flow by itself establishes a self-organized dynamic structure[6] (not to be confused with the "self-assembly" of complex spatial structures, even though this is also sometimes called "self-organization" in the chemical literature). Here, the TBM is augmented by the inclusion of tracer contaminants subject to degradation; the resulting model is a complex and self-organizing (in the sense discussed in ref 6) chemical reaction network, in which the microbial degradation sites are strongly coupled to the flow because they are dynamically activated or deactivated depending upon the contaminant concentration. Consequently, predicting the contaminant fate for a given degradation rate is complicated, so we rely here upon computations for our first study of such a model.

Of the large effort and literature on this problem, the following recent work on models[4,5,7,8] and experiments[9−13] dealing with fracture flows, and on models[2,3] and experiments[1,14−16] of microbial degradation in the subsurface, provides a context for this study. There is such a wide variety of biogeochemical scenarios in which biodegradation can occur that we ask, "To what extent can scale-free generalizations about such processes can be drawn?" With this question in mind, we present here a simple (possibly the simplest) model of the complicated (and possibly complex) biodegradation scenario in fractured media. The scale-free nature of the sandpile model[6] that underlies our work suggests that the insight extracted from it may be broadly applicable. Our primary interest is to determine the sensitivities to variations in the degradation in a simply understood model, as a first step to bounding the range of behavior in more realistic scenarios.

This variant of the TBM employs the following assumptions, the first set concerning the microorganisms and the second concerning the flow. First, we assume that microbial contaminant degradation is due to microorganisms that (i) are pervasive and long-lived in the subsurface, (ii) employ organic contaminants as part (or all) of their food source, (iii) become dormant, isolated, and possibly planktonic when the food source is low, under which conditions they do not significantly degrade the contaminant, but (iv) become active and effectively degrade the contaminant if they can form communities when the food source becomes sufficiently rich. We modeled the degradation with

† Part of the special issue "Frank H. Stillinger Festschrift".

* Author to whom correspondence should be addressed. E-mail: yaq@inel.gov.

10.1021/jp0476500 CCC: $27.50
Published on Web 11/09/2004

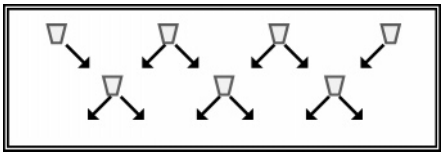

Figure 1. Fragment of the TBM network. The arrows indicate the direction of the flow when the bucket is tipped.

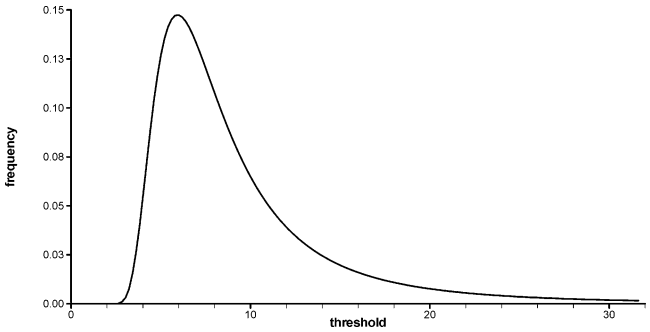

Figure 2. The Frechet distribution (eq 1) for the thresholds. The distribution has both a mean and a standard deviation of 10.

approximately first-order kinetics at low concentrations, at each degradation site (or trap). We chose first-order kinetics because it is common for biodegradation reactions with low concentrations of contaminant. Instead of saturating with zeroth-order kinetics at high concentrations (as in Michaelis−Menten kinetics), we assume that the microorganisms are poisoned and degradation ceases from those sites. These assumptions have been discussed in the literature, for example, refs 2 and 14−16. Second, we assume that the flow in fractured media can be convergent as well as divergent. The hypothesis of convergent flow the former has only recently received experimental evidence,[10] while divergent flow is the more common circumstance. We will consider contaminant degradation in both convergent and divergent flows.

TABLE 1: Active Trap Populations and Drip Contaminant Concentrations[a]

	parameters		traps (%)		concentrated × 10^3	
case	Φ	Ω	μ	2σ	μ	2σ
1	0.0		41	18	9.2	3
			10	8	6.2	2
2	0.8		28	8	10	5
			10	6	7	4
3	1.0	8	44	14	9.8	2
			13	8	7.5	2
4	1.0	20	20	4	23	54
			18	4	20	54

[a] The first column labels the cases, according to the combination of Φ and Ω parameters employed. The μ and σ are the sample means and standard deviations, respectively. For each case, the top and bottom rows correspond to the slow ($\gamma = 10^{-4}$) and the fast ($\gamma = 10^{-3}$) degradation rates, respectively. The left-hand pair of the (μ, 2σ) columns displays results for the active trap population, expressed as the percent of the total number of buckets. The right-hand pair displays results for the contaminant concentration of the drips, multiplied by 1000. The shading indicates exceptions to the otherwise normal distribution of the fluctuations.

2. Description of the Chemical Reaction Network Model. *2.A. Description of the "Tipping Bucket" Model for the Fracture Flow.* The "tipping bucket model" (TBM) is a cellular automaton similar to the generic directed "sandpile" model[6,17,18] but with the added complications of stochastic singly directed flow and dynamic overloading.[4,5] The TBM idealizes the fracture network as a regular, two-dimensional array of intersections arranged on a diamond lattice (Figure 1). Here, we implemented periodic boundary conditions along the vertical edges of the network of 50 (horizontal) × 1000 (vertical) buckets. The Φ parameter is defined as the fraction of intersections, or buckets, that are connected to only one or the other but not both of the neighboring buckets in the row below. $\Phi = 0$ corresponds to a maximally biconnected network, while for $\Phi > 0$, the choice

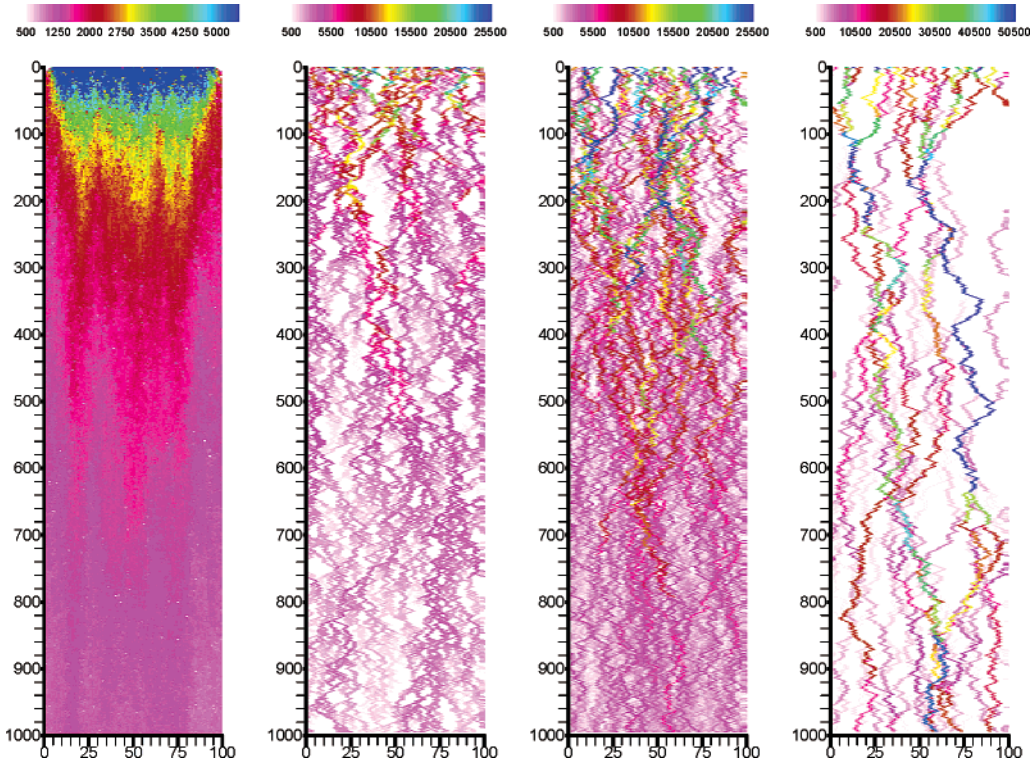

Figure 3. Cumulative number of bucket tips for eight million spills. The four panels correspond to cases 1−4, left to right. The color legends indicate the cumulative number of tips for each bucket and vary between the panels, e.g., the leftmost panel would be all magenta on the scale of the next three panels.

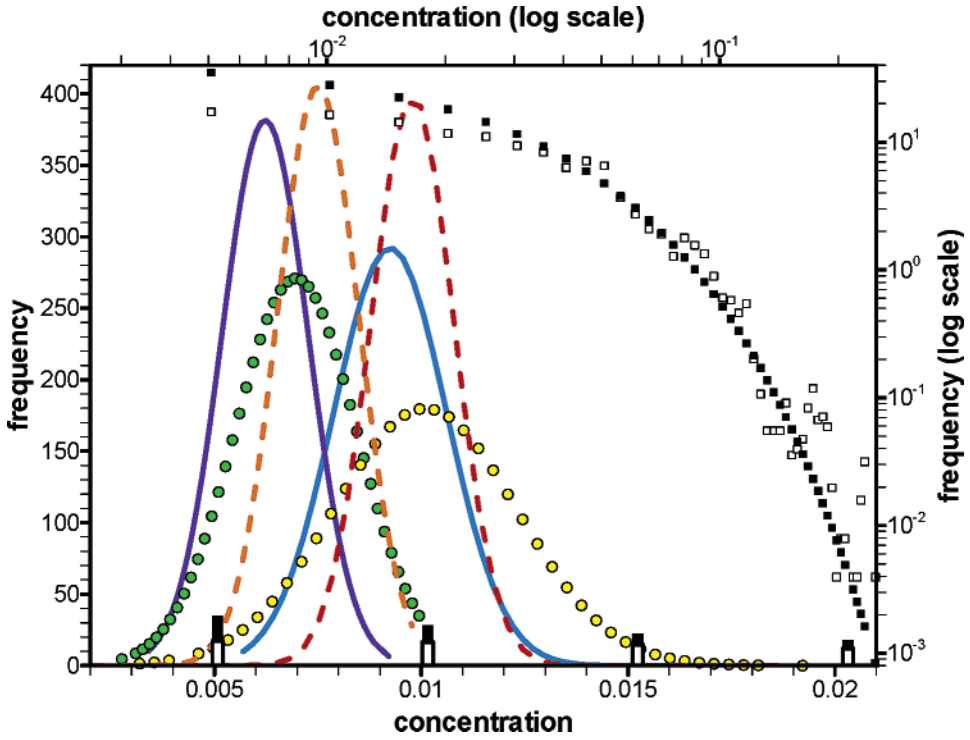

Figure 4. The distribution of contaminant concentration in the exiting drips. The bottom and left axes portray the results on a linear scale corresponding to the "slow" and "fast" degradation rates, respectively: blue and violet (solid) for case 1, yellow and green (circles) for case 2, red and orange (dashed) for case 3, and black and white (bars) for case 4. The results for cases 1−3 correspond to fits of the normal distribution to the first two moments (Table 1); the results for case 4 are raw bins from the histogram. The right and top axes portray the same results for case 4 (squares) on a log−log scale.

of which of the two neighboring buckets to connect is random; once chosen, it remained set for the duration of the simulation. We added one unit of water to a randomly chosen bucket on the top row of the network. Each addition corresponds to one unit time step. Between additions (or spills), the network is relaxed by tipping the eligible buckets as follows: when the level of water in a bucket j exceeds its threshold θ_j, it tips and distributes all of its volume to the (one or two) connecting buckets in the row below; the direction of the flow is always top to bottom. The relaxation process itself (i.e., the tipping of the eligible buckets) is considered to be virtually instantaneous compared with the interval between the spills and will not be included in the dynamics that we measure; the dynamics of the flow and reaction kinetics described below in 2.B are measured only between spills. For convenience in the analysis, we take the interval between each spill to be the same.

In ref 4 all of the thresholds were set equal to 10, but in ref 5 the added realism of spatially (but not temporally) variable bucket thresholds within the network was found to be useful, so we employ the same distribution here. The θ_j here were assigned to each bucket (to remain fixed thereafter), without spatial correlation, by randomly sampling from the Fréchet distribution f, that is, for $\theta \geq 0$,

$$f(\theta) = (\beta/\theta)(\alpha/\theta)^{\beta} \exp\{-(\alpha/\theta)^{\beta}\}; \alpha, \beta > 0 \qquad (1)$$

This unimodal distribution is a member of the "generalized extreme value" family of distributions and happens also to possess convenient scaling properties. Its essential singularity at the origin ensures a smooth, rapid approach to zero density there. Its algebraic decay for large thresholds is physical: the diameter of the fracture aperture is a primary factor for the threshold,[5,7−13] while experiments indicate that the distribution of fracture apertures has a power-law tail.[19] Here, we considered only one set of parameters ($\alpha = 6.76396$ and $\beta = 2.52996$) for the Fréchet distribution, which resulted from setting both the mean threshold ($\mu_\theta = 10$) and its standard deviation ($\sigma_\theta = 10$). Figure 2 shows the resulting threshold distribution.

Dynamic overloading occurs when a large volume of fluid is passed to a small volume intersection and causes the bucket to split its flow to both intersections (buckets) in the row below it, even if normally it would only direct the flow singly, that is, to only one intersection (bucket) in the row below. Overloading has been observed in experiments.[11] The TBM was first augmented with an overload process in ref 5, and we do so here, for added realism, by introducing a second threshold condition at each bucket through introduction of the overload parameter $\Omega \geq 1$, constant for the entire network. For each bucket j, if the bucket receives a load L_j that is larger than θ_j by a factor of Ω, that is, if $L_j > \Omega \times \theta_j$, then the restriction to flow into only one bucket below (if any) is overridden for that instance only, so that both of the left and right connecting buckets below equally receive one-half L_j from j.

We found in ref 5 that as occurrence of dynamic overloading increases, the model behavior transitions from convergent flow back to divergent flow comparably to that found in ref 4 for variations with Φ. The divergent flow with overloading differs from that for Φ as overloading occurs as a natural consequence of a heterogeneous field and imposes a dynamic structure where additional pathways activate or deactivate in time.

The TBM provides a driven flow in fractured media that becomes a self-organized dynamic structure.[4−6] With the overload process, it exhibits a natural transition between divergent and convergent flow.[4,5] In the next subsection, we discuss the addition of chemical reactions to the TBM, which represent the microbial degradation of contaminant, but could easily be adapted for other models (for example, others recently

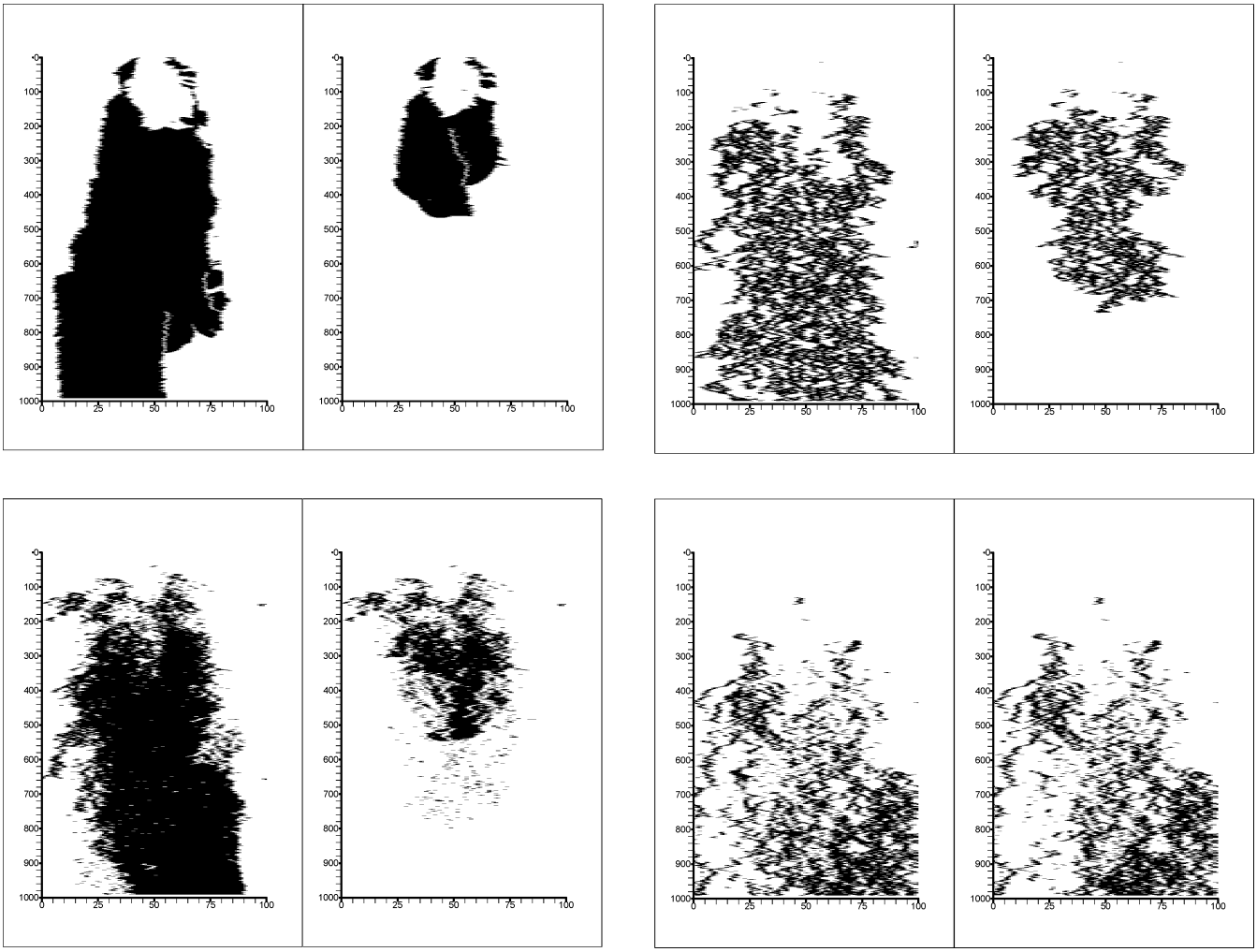

Figure 5. Snapshot of the distribution of traps. Panels (a−d) correspond to cases 1−4, respectively. The black pixel corresponds to the presence of an active trap on the network at the end of the simulation. The left- and right-hand side of each panel corresponds to the low and high degradation rate, respectively.

have constructed self-organized chemical reaction networks in different contexts).[20,21]

2.B. Description of the Contaminant Degradation Model. With the addition (or spill) of one unit of water to a randomly chosen bucket on the top row, we also added one unit of contaminant (a tracer that does not interfere with the flow), but it was added only to the central bucket on the top row, and only if that bucket also had been chosen to receive the added water. The contaminant was quickly diluted into the network and achieved steady state in the presence of degradation. We modeled the contaminant degradation by initially placing one trap in each bucket that, when active, removed contaminant from the bucket via approximate first-order kinetics as follows: the contaminant in each bucket with a trap was reduced by a factor of $(1 - \gamma)$, where $\gamma = 10^{-4}$ for *slow* degradation, or $\gamma = 10^{-3}$ for *fast* degradation, at every spill, irrespective of the amount of water in the bucket, or whether the bucket had been tipped. The rate γ has dimensions of inverse time (set by the interval between additions of water) but here, as with all parameters, it has reduced units, that is, all units are unity. For both of these values, $(1 - \gamma)$ reasonably approximates the factor $\exp(-\gamma)$ that would result from exact first-order kinetics,[16] while it significantly reduces the computational burden of the simulation. The trap is reversibly deactivated whenever the contaminant in that bucket falls below the activation concentration of 0.01 and irreversibly deactivated whenever the contaminant rises above the toxic concentration of 0.05. All four of these parameters (with no dimensions attached) were chosen for our convenience, so that the behavior could be observed on a scale of 10^6 spills; the parameters were fixed during each simulation.

3. Results

We examined only the cases with random branching fraction $\Phi = 0.0$ (case 1), $\Phi = 0.8$ (case 2), and $\Phi = 1.0$; for the latter, we examined only the cases with overload parameter $\Omega = 8$ and $\Omega = 20$ (cases 3 and 4, respectively). We always discarded the results of the first 10^6 spills; all of the following results were taken from subsequent runs of 8×10^6 spills.

Cases 1−3 support divergent flow, while case 4 supports convergent flow.[5] One of the symptoms of convergent flow is evident in Figure 3, where in the far right panel, there are channels that each accumulates substantially more flow (as indicated by the cumulative number of times a bucket was tipped) than the lower-flux channels above them. The trap population and the contaminant concentration in the drips, though always fluctuating, achieved a steady state in less than 10^5 spills under these conditions; the steady-state dynamics for each were essentially Brownian (or ARMA), since they possess Hurst exponents in the range 0.45−0.55 (a Hurst exponent of one-half corresponds exactly to Brownian motion).[22] We compared the results for the slow and fast degradation rates γ

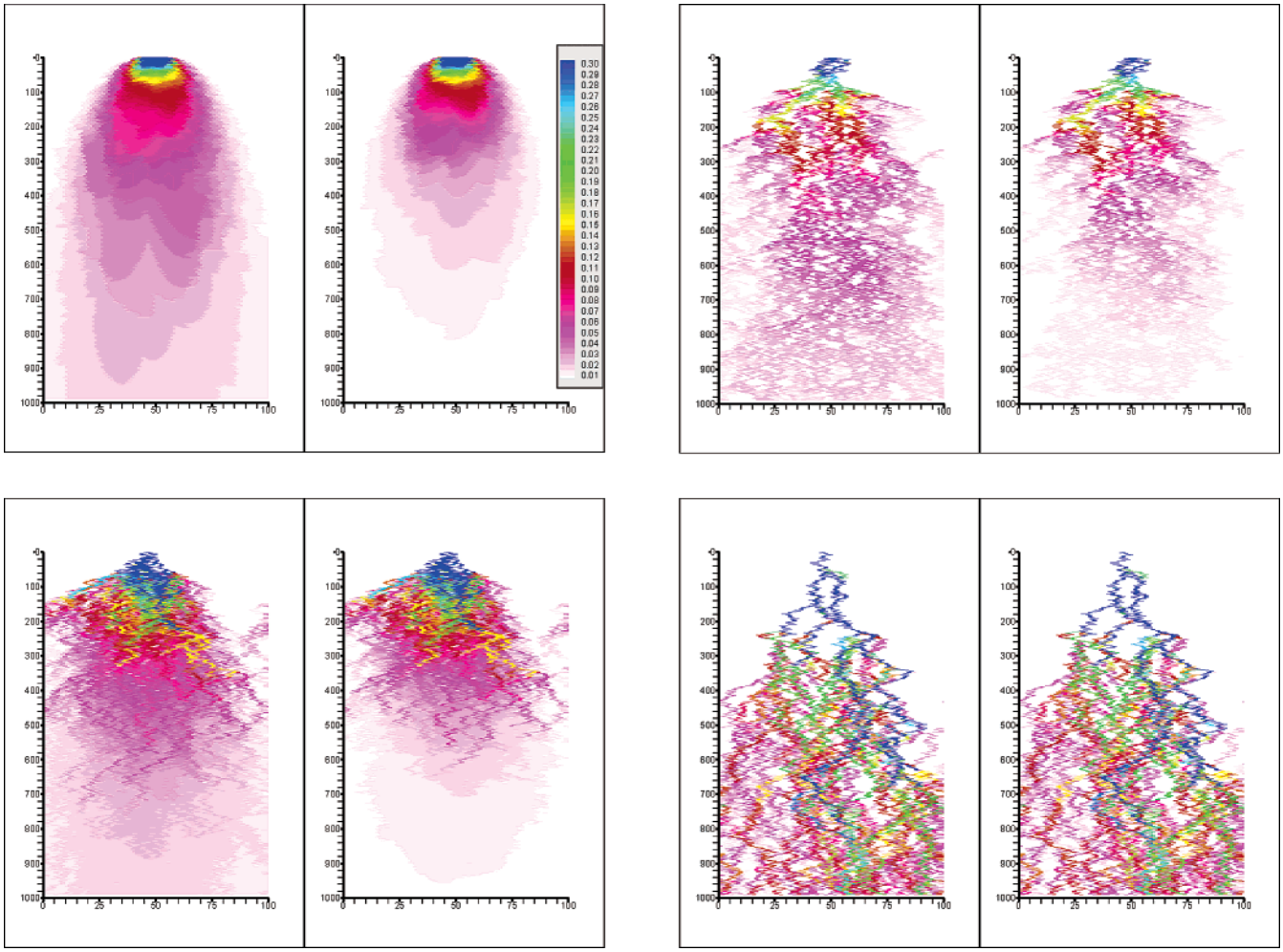

Figure 6. Maximum concentration of contaminant. Panels (a−d) correspond to cases 1−4, respectively. The color legend in panel a is the same for all the panels in this figure. The maximum concentration was recorded for each bucket before it tipped (if it tipped). The left- and right-hand side of each panel corresponds to the low and high degradation rate, respectively.

(see 2.B above) for each of cases 1−4. The resulting sample means and standard deviations are listed in Table 1.

The fluctuations of the total amount of water in the system were also large but were normally distributed for all cases and were not included in Table 1; trapping does not affect the distribution of the water, only of the contaminant. The fluctuations of the steady-state trap populations are large but normally distributed with one exception: in case 1, for the fast degradation rate, its slightly asymmetric fluctuations are much better approximated by the gamma distribution that matches the first two moments, but we have no explanation for this behavior, except that it was not the result of deviation from the steady state. The trap population in case 4 changes very little despite an order of magnitude increase in the degradation rate, while the trap populations are significantly affected by the change in degradation rates in the other cases.

The contaminant concentrations in the drips are well approximated by the normal distribution for cases 1−3, as indicated in Figure 4. As also indicated in Figure 4, for both results in case 4, (shaded in Table 1), the first two moments are not enough to characterize their distribution, which has a long tail (that decays as either a stretched exponential or a power law with an exponential rolloff),[6] of the contaminant concentration. An order-of-magnitude increase in the decay rates lowers the concentration in the drips by only about one-third for case 1; overloading in case 3 provides results similar to the maximally connected case 1, while without significant overloading, case 4 produces an insignificant change in the contaminant concentration in the drips even with an order of magnitude increase in the decay rate. Increasing the degradation rate by an order of magnitude for case 2 produces a decrease in the contaminant concentration comparable to cases 1 and 3 but with much larger fluctuations and therefore of less statistical significance. We recall that cases 1−3 support diverging flow while case 4 supports converging flow.

The trap population results displayed in Table 1 do not show their spatial distribution; these are represented in Figure 5 with snapshots of the trap distributions for the four cases with the two degradation rates. The introduction of the toxic threshold accounts for the unoccupied space near the source of the contaminant, where otherwise most of the traps would be found. The traps with the lower degradation rates are the more widely distributed, as expected.

The maximum contaminant concentration experienced by a bucket during the simulation is presented in Figure 6. As in Table 1, case 1 reflects the impact of the increased degradation rate more strongly than case 2, while in case 4 there is no discernible impact. Case 3 shows the importance of overloading the minimally connected geometry, with which results similar to those of case 1 are obtained. Cases 1−3 show that the contaminant plume is effectively bounded or contained in divergent flow, but case 4 shows that the contaminant plume is not contained at all in the convergent flow.

4. Conclusions

We simulated a chemical reaction network with feedback, in a driven flow described by self-organized "tipping bucket" model with distributed and dynamically overloaded thresholds. We found here that an order-of-magnitude increase in the degradation rate of the individual, dynamic traps in the flow translated into much smaller increases in the overall reduction of contaminant concentration in the exiting flow. The strongest reductions in contaminant concentration, up to one-third, were found in the systems (cases 1−3) that supported diverging flow, while the weakest, almost negligible reduction was found in the system (case 4) that supported converging flow.

Acknowledgment. This work was supported by the INEEL Environmental Systems Research and Analysis Program and the Environmental Management Science Program, Office of Environmental Management, U. S. Department of Energy. The Idaho National Engineering & Environmental Laboratory is operated for the U.S. Department of Energy under DOE-ID Operations Office Contract DE-AC07-99ID13727. Sandia National Laboratories is operated for the U.S. Department of Energy under DOE-AL Operations Office Contract DE-AC04-94AL85000.

References and Notes

(1) Stoner, D. L.; Stedtfeld, R. D.; Tyler, T. L.; White, F. J.; McJunkin, T. R.; LaViolette, R. A. *Geophys. Res. Lett.* **2003**, *30*, 1960; http://dx.doi.org/10.1029/2003GL017860.

(2) LaViolette, R. A.; Watwood, M. E.; Ginn, T. R.; Stoner, D. L. *J. Phys. Chem. A* **1999**, *103*, 4480.

(3) Dunlap, D. H.; LaViolette, R. A.; Parris, P. E. *J. Chem. Phys.* **1994**, *100*, 8293.

(4) Glass, R. J.; LaViolette, R. A. *Geophys. Res. Lett.* **2004**, *31*, L15501; http://dx.doi.org/10.1029/2004GL019511.

(5) LaViolette, R. A.; Glass, R. J. *Geophys. Res. Lett.* **2004**, *31*, L18501; http://dx.doi.org/10.1029/2004GL020659.

(6) Jensen, H. J. *Self-Organized Criticality: Emergent Complex Behavior in Physical and Biological Systems*; Cambridge University Press: New York, 1998.

(7) Glass, R. J.; Nicholl, M. J.; *Geophys. Rev. Lett.* **2004**, *31*, L06502; http://dx.doi.org/10.1029/2003GL019252.

(8) Glass, R. J.; Rajaram, H.; Detwiler, R. L. *Phys. Rev. E* **2003**, *68*, 061110.

(9) Wood, T. R.; Glass, R. J.; McJunkin, T. R.; Podgorney, R. K.; LaViolette, R. A.; Noah, K. S.; Stoner, D. L.; Starr, R. C.; Baker, K. *Vadose Zone J.* **2004**, *3*, 90; http://vzj.scijournals.org/cgi/content/abstract/ 3/1/90?etoc.

(10) LaViolette, R. A.; Wood, T. R.; McJunkin, T. R.; Noah, K. S.; Podgorney, R. K.; Starr, R. C.; Stoner, D. L.; Glass, R. J. *Geophys. Res. Lett.* **2003**, *30*, 1083; http://dx.doi.org/10.1029/2002GL015775.

(11) Glass, R. J.; Nicholl, M. J.; Rajaram, H.; Wood, T. R. *Water Resour. Res.* **2003**, *39*, 1352;. http://dx.doi.org/10.1029/2003WR002015.

(12) Glass, R. J.; Nicholl, M. J.; Pringle, S. E.; Wood, T. R. *Water Resour. Res.* **2002**, *38*, 1281; http://dx.doi.org/10.1029/2001WR001002.

(13) Wood, T. R.; Nicholl, M. J.; Glass, R. J. *Geophys. Res. Lett.* **2002**, *29*, 2191; http://dx.doi.org/ 10.1029/2002GL015551.

(14) Lehman, R. M.; O'Connell, S. P. *Appl. Environ. Microbiol.* **2002**, *68*, 1569.

(15) Lehman, R. M.; Colwell, F. S.; Bala, G. A. *Appl. Environ. Microbiol.* **2001**, *67*, 2799.

(16) Alexander, M. *Biodegradation and Bioremediation*; Academic Press: New York, 1994.

(17) Dhar, D.; Ramaswamy, R. *Phys. Rev. Lett.* **1989**, *63*, 1659.

(18) Dhar, D. *Physica A* **1999**, *263*, 4.

(19) Bonnet, E.; Bour, O.; Odling, N. E.; Davy, P.; Main, I.; Cowie, P.; Berkowitz, B. *Rev. Geophys.* **2001**, *39*, 347.

(20) Santra, S. B.; Sapoval, B. *Physica A* **1999**, *266*, 160.

(21) Gaveau, B.; Latermoliere, D.; Moreau, M. *J. Chem. Phys.* **2003**, *118*, 5754.

(22) Salas, J. D.; Delleur, J. W.; Yevjevich, V.; Lane, W. L. *Applied Modeling of Hydrologic Time Series*; Water Resources Publications: Littleton, CO, 1980.